# Crystal Structure of a Carbon Monoxide Dehydrogenase Reveals a [Ni-4Fe-5S] Cluster

Holger Dobbek,[1*] Vitali Svetlitchnyi,[2*] Lothar Gremer,[2] Robert Huber,[1] Ortwin Meyer[2,3*]

The homodimeric nickel-containing CO dehydrogenase from the anaerobic bacterium *Carboxydothermus hydrogenoformans* catalyzes the oxidation of CO to $CO_2$. A crystal structure of the reduced enzyme has been solved at 1.6 angstrom resolution. This structure represents the prototype for Ni-containing CO dehydrogenases from anaerobic bacteria and archaea. It contains five metal clusters of which clusters B, B′, and a subunit-bridging, surface-exposed cluster D are cubane-type [4Fe-4S] clusters. The active-site clusters C and C′ are novel, asymmetric [Ni-4Fe-5S] clusters. Their integral Ni ion, which is the likely site of CO oxidation, is coordinated by four sulfur ligands with square planar geometry.

The capacity to oxidize carbon monoxide (CO) is a central metabolic feature of several groups of bacteria and archaea. CO is used as a growth substrate by the aerobic carboxidotrophic bacteria, species of the anaerobic acetogenic bacteria, sulfate-reducing bacteria and archaea, phototrophic bacteria, methanogenic archaea, and hydrogenogenic bacteria (*1–4*). *Carboxydothermus hydrogenoformans*, the most extensively studied representative of the hydrogenogenic bacteria, couples the oxidation of CO to $CO_2$ with the reduction of protons to $H_2$ in the energy-conserving reaction $CO + H_2O \rightarrow CO_2 + H_2$, $\Delta G^{\circ\prime} = -20$ kJ mol$^{-1}$ (*4*, *5*).

Carbon monoxide dehydrogenases (CODHs), the enzymes responsible for CO metabolism in microorganisms, all formally catalyze the same reaction: $CO + H_2O \rightarrow CO_2 + 2e^- + 2H^+$. Two principal types of CODHs have been defined: Mo–[2Fe-2S]–FAD CO dehydrogenases from aerobic bacteria (*3*), and Ni–[4Fe-4S] CODHs from anaerobic bacteria (*1*, *2*, *5*, *6*). Some of the latter operate in a complex with acetyl-CoA synthase (ACS).

Crystal structures were first reported for Mo CODHs from the aerobic carboxidotrophic bacteria *Oligotropha carboxidovorans* and *Hydrogenophaga pseudoflava* (*3*, *7*, *8*). The Mo CODHs are composed of an FeS protein, containing type I and type II [2Fe-2S] clusters; a flavoprotein, binding the FAD cofactor; and a Mo protein, which carries the molybdopterin-cytosine dinucleotide (MCD)-containing CO oxidation site.

*Carboxydothermus hydrogenoformans* contains two homodimeric Ni CODHs, which are associated with the inner aspect of the cytoplasmic membrane (*5*). Both CODHs are monofunctional; they have no ACS activity. The electrons supplied by CODH I drive the translocation of protons across the cytoplasmic membrane by a complex I–related hydrogenase. CODH II has a key function in the supply of reducing power and $CO_2$ for carbon assimilation. Both *C. hydrogenoformans* CODHs show high sequence similarity to the monofunctional CODH from the phototroph *Rhodospirillum rubrum* and the CO-oxidizing β-subunit of the bifunctional CODH/ACS from the acetogen *Clostridium thermoaceticum* (*9*).

The holoenzymes CODH I (137.0 kD; protein subunit, 67.5 kD) and CODH II (136.6 kD; protein subunit, 67.3 kD) contain (atoms per mole of subunit) about 1 Ni, 10 Fe, and 11 labile sulfurs per monomer, as determined by inductively coupled plasma mass spectroscopy, neutron activation, and chemical analysis. Electron paramagnetic resonance (EPR) spectroscopy indicates [4Fe-4S] clusters and EPR-silent Ni, interpreted as a $Ni^{2+}$ ion.

Previous work on the CODHs from *R. rubrum* or *C. thermoaceticum* has identified a mixed Ni-Fe cluster (cluster C) and a conventional cubane-type [4Fe-4S] cluster (cluster B) [for review, see (*2*)]. It has been proposed that cluster C is composed of an [4Fe-4S] cluster containing a pentacoordinated Fe atom that is bridged to the Ni atom by an unidentified ligand "X" (*10*). Another model structure proposes a binuclear [Fe-Ni] cluster that is bridged by two cysteines and is coordinated via its Fe atom and an unknown ligand "X" with [4Fe-4S] (*11*, *12*).

Here, we describe the three-dimensional structure of the Ni CODH II from *C. hydrogenoformans* as determined by x-ray crystallography to a resolution of 1.63 Å. This shows the positions and coordinations of the five metal clusters of the dimeric enzyme and reveals a [Ni-4Fe-5S] cluster in the active site. *C. hydrogenoformans* CODH II is a prototype of the entire class of Ni-containing CODHs from anaerobic bacteria and archaea.

**Overall structure.** The structure of the *C. hydrogenoformans* CODH II was solved by multiple wavelength anomalous dispersion (MAD) methods (*13*) as described in Table 1 and has been refined to 1.63 Å resolution (Table 2). The overall dimensions of dimeric CODH are 88 × 63 × 60 Å with an accessible surface area of 37,300 Å$^2$ (Fig. 1). The enzyme has a mushroom shape of two identical, intertwined subunits that are covalently linked.

The dimeric enzyme coordinates five metal clusters (Fig. 1). Each subunit contains a mixed-type cluster composed of Ni, Fe, and S (cluster C or C′) along with a conventional cubane-type [4Fe-4S] cluster (cluster B or B′). An additional [4Fe-4S] cluster (cluster D) is bound at the subunit interface. The presence of one, but not two, types of clusters in addition to cluster C has been reported on the basis of spectroscopic results [for review, see (*2*)]. Our proposed assignment of the two identical [4Fe-4S] clusters as cluster B, and of the [4Fe-4S]

**Table 1.** Data and wavelength statistics.

| Parameter | Data | | | |
|---|---|---|---|---|
| Wavelength (Å) | 1.7389 | 1.7422 | 1.4856 | 1.5418 |
| Resolution limits (Å) | 30–2.5 | 30–2.5 | 30–2.1 | 19–1.63 |
| Completeness (%) | 97.3 | 96.9 | 95.1 | 99.7 |
| $R_{merge}$ (%)* | 3.4 | 3.4 | 3.6 | 5.2 |
| $f'$ | −5.8 | −8.2 | −0.8 | |
| $f''$ | 4.1 | 2.5 | 2.9 | |
| Phasing power$_{iso}$† | 3.7 | 3.7 | | |
| Phasing power$_{ano}$‡ | 2.1 | 2.3 | 2.0 | |
| $R_{Cullis}$§ | 40.5 | 30.9 | | |

*$R_{merge} = \Sigma_{hkl}|\langle I\rangle - I|/(\Sigma_{hkl} I)|$. †Isomorphous phasing power $= \Sigma_n|FH|/\Sigma_n|E|$, where FH is the calculated structure-factor amplitude of the heavy-atom structure and $E$ is the residual lack of closure. ‡Anomalous phasing power $= 2\Sigma_n|F^-H|/\Sigma_n|E|$, where $|F^-H|$ is the anomalous-contribution amplitude. §$R_{Cullis} = \Sigma_{hkl}||FPH \pm FP| - FH(Calc)|/\Sigma_{hkl}|FPH \pm FP|$ for centric reflections and isomorphous contributions.

[1]Max-Planck-Institut für Biochemie, Abteilung Strukturforschung, Am Klopferspitz 18a, D-82152 Martinsried, Germany. [2]Lehrstuhl für Mikrobiologie and [3]Bayreuther Zentrum für Molekulare Biowissenschaften (BZMB), Universität Bayreuth, D-95440 Bayreuth, Germany.

*To whom correspondence should be addressed. E-mail: dobbek@biochem.mpg.de, vitali.svetlitchnyi@uni-bayreuth.de, ortwin.meyer@uni-bayreuth.de.

cluster in the interface as the new cluster D, does not necessarily coincide with the spectroscopic cluster B and is retained to conform to the traditional nomenclature.

Each subunit comprises three domains, the $NH_2$-terminal, the middle, and the COOH-terminal domain (Fig. 2). The $NH_2$-terminal domain (residues 4 to 237) is predominantly α-helical and can be separated into two functional subdomains. The first subdomain (residues 3 to 72) contains two binding regions for clusters B and D (Fig. 2). Three $NH_2$-terminal α helices are followed by a small double-stranded β sheet, which contributes to binding the two [4Fe-4S] clusters, as well as separating them. Cluster D establishes the covalent link between the two monomers. It lies on the crystallographic two-fold axis relating the subunits and is coordinated to each through $Cys^{39}$ and $Cys^{47}$. Cluster B (or B′) is coordinated by $Cys^{48}$, $Cys^{51}$, $Cys^{56}$, and $Cys^{70}$, corresponding to a binding motif of $CysX_2CysX_4CysX_{13}Cys$, which is similar to the binding motif characteristic of low-potential [4Fe-4S] ferredoxins ($CysX_2CysX_2CysX_nCys$) (*14*). The homodimer is created by an approximately orthogonal interaction between this three-helix bundle and its symmetrical partner, and the covalent linkage through cluster D. The tight association of the dimer is illustrated by its extensive interface, which covers about 16% of the total accessible surface of the monomer. The middle and the COOH-terminal domains both show a Rossmann-fold topology and superpose with a root mean square (rms) deviation of 1.7 Å.

**Active site cluster.** The mixed-type Ni-Fe clusters C and C′ in *C. hydrogenoformans* CODH appear to be the active sites of CO oxidation (Fig. 3). This view agrees with genetic evidence and extensive kinetic, electron nuclear double-resonance (ENDOR) spectroscopy, and rapid freeze-quench EPR studies by several groups on the CODHs from *R. rubrum* and *C. thermoaceticum* (*2*, *10*, *15–17*). In the CODH from *C. hydrogenoformans*, cluster C is located about 18 Å below the protein surface close to the subunit interface. Cluster C contains one Ni atom, four Fe atoms, and five labile sulfur atoms, which are arranged as an asymmetrical heteronuclear [Ni-4Fe-5S] cluster (Fig. 3). The metal ions of the cluster are covalently bound to the protein by five cysteine residues and one histidine residue, which originate from the middle ($Cys^{295}$, $Cys^{333}$, $His^{261}$) and COOH-terminal ($Cys^{446}$, $Cys^{476}$, $Cys^{526}$) domains. All Fe atoms of the cluster are tetrahedrally coordinated. The geometry of a [3Fe-3S] subsite assembled by Fe2, Fe3, and Fe4 and three $\mu_3$-S atoms of cluster C (Fig. 3A) approximates the corresponding geometry of a cubane-type [4Fe-4S] cluster. Fe1 is unusually coordinated by Sγ of $Cys^{295}$ and Nε2 of $His^{261}$ (Fig. 3A). The distances between the irons in the [3Fe-3S] subsite, which range from 2.6 to 2.8 Å, are similar to those usually found in [2Fe-2S], [3Fe-4S], and [4Fe-4S] clusters. The sequestered position

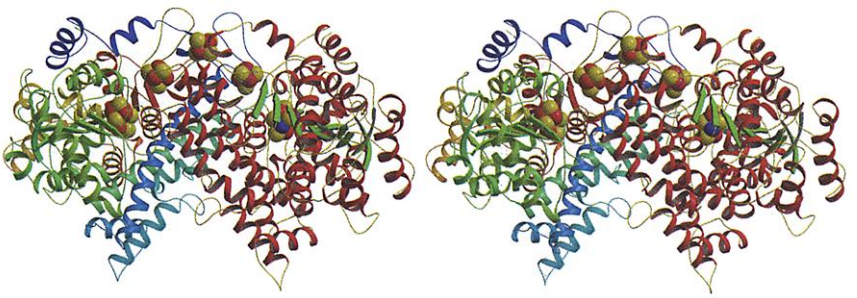

**Fig. 1.** Stereo presentation of the CODH II dimer of *Carboxydothermus hydrogenoformans*. The subunits are colored differently. The left subunit is colored from blue at the $NH_2$-terminus via green through yellow to red at its COOH-terminus. The right subunit is colored according to its secondary structure, with red for α helices and green for β sheets. Figures 2, 3, and 5 were also created by using BOBSCRIPT (*36*) and RASTER3D (*37*).

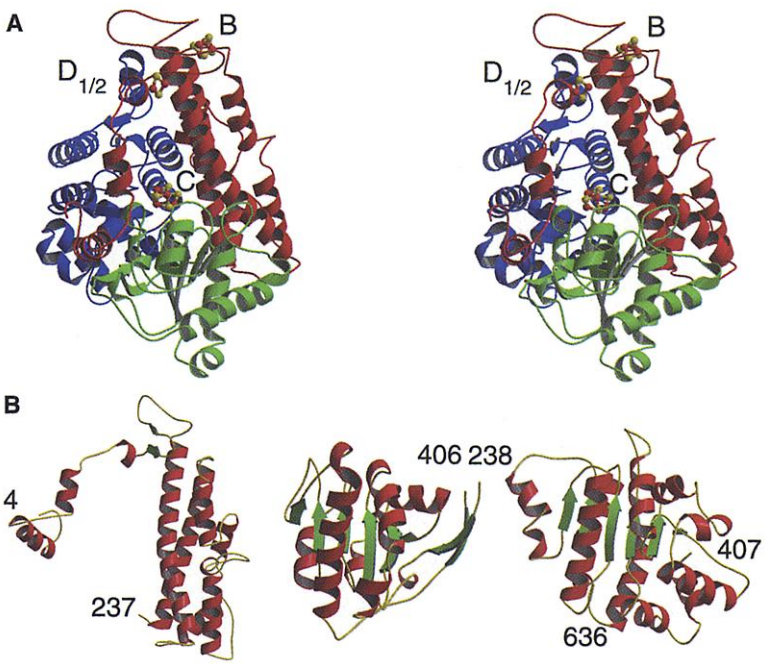


**Fig. 2.** Fold topology of the CODH II monomer. (**A**) Stereoview of one subunit. The subunit can be divided into three domains. The $NH_2$-terminal domain shows a predominantly α-helical fold and is depicted in red. The two [4Fe-4S] clusters B and D are bound by the $NH_2$-terminal domain. Only one-half of cluster D is shown, as the complete cluster is shared between the monomers. Cluster C is coordinated by residues of the middle (green) and the COOH-terminal domain (blue) and is close to the interface of the three domains. (**B**) Isolated domains ($NH_2$-terminal, middle, and COOH-terminal domain from left to right) are colored according to their secondary structure. These domains are oriented differently from those in (A) in order to display their arrangement of secondary structure elements. $NH_2$- and COOH-terminal residues of the domains are marked by the corresponding sequence numbers.

**Table 2.** Refinement statistics.

| Parameter | Value |
|---|---|
| No. of measured reflections* | 196,092 |
| No. of independent reflections | 57,646 |
| Resolution range (Å) | 19–1.63 |
| No. of nonhydrogen atoms | 5435 |
| Protein residues | 633 |
| Water molecules | 838 |
| $I/\sigma(I)$ overall (1.72–1.63 Å) | 9.8 (1.9) |
| Crystallographic *R*-factor | 16.1 |
| Free *R*-factor† | 20.9 |
| Average B-factor for protein (Å²) | 17.8 |
| r.m.s.d. in bond lengths (Å) | 0.006 |
| r.m.s.d. in bond angles (°) | 1.9 |
| r.m.s.d ΔB (Å²) | 4.6 |

*In the data set used for refinement, collected at λ = 1.5418 Å, Friedel mates were merged for refinement. †The free *R*-factor was calculated from 3% of the data, removed at random before the refinement was carried out. r.m.s.d., root mean square deviation.

of Fe1 in cluster C is apparent from nearest Fe-Fe distances of 3.3 Å and a distance of 2.8 Å to the Ni (Fig. 3B).

The Ni ion is an integral constituent of cluster C (Fig. 3). It is coordinated by four S atoms and shares two inorganic $\mu_3$-S atoms and one $\mu_2$-S atom with the four Fe atoms of the cluster. $Cys^{526}$ donates the fourth S-ligand to the Ni ion and completes the slight tetrahedrally distorted square-planar geometry. The Ni ion lies about 0.3 Å above the center of the plane spanned by its four ligands. Observed Ni-S bond lengths are all ~2.3 Å. The integration of Ni in cluster C is also evident from the short distances of ~2.8 to 2.9 Å between Ni and Fe1 and Ni and Fe3. The square-planar geometry of the metal ligands in cluster C is characteristic of electronic configurations of $3d^8$, with the most prominent example, $Ni^{II}$ (*18*). Its four similar ligands strongly suggest a low-spin $Ni^{II}$ state, which is supported by a diamagnetic EPR silent $Ni^{2+}$ ion in all oxidation states of CODH II (*5*).

Previous models proposed for the Ni-Fe clusters in the CODHs from *R. rubrum* (*10*–*12*) or *C. thermoaceticum* (*10*) essentially assume a cubane-type [4Fe-4S] cluster to which an outside Ni ion is indirectly ligated. In contrast, Ni is an integral constituent of cluster C of the CODH from *C. hydrogenoformans*, with all four Fe atoms bridged to the Ni ion by labile sulfur ligands (Fig. 3). The geometry and arrangement of cluster C thus differ substantially from the models and have not been previously observed in biological metal clusters (*19*, *20*); although it has been shown for sulfite reductase (*21*) and Fe-only hydrogenase (*22*) that a covalent linkage of a cubane-type [4Fe-4S] cluster to another metal-containing prosthetic group is possible. No ordered nonprotein ligands in addition to labile sulfur were observed coordinating any of the Fe atoms of cluster C of the dithionite-reduced CODH from *C. hydrogenoformans* (Fig. 3).

**Active site environment.** In addition to the six residues binding cluster C, other highly conserved residues in the vicinity of the cluster are likely essential in defining the active-site environment (*23*). This applies to $Lys^{563}$ in hydrogen-bonding distance to $\mu_2$-S between Ni and Fe1, and to $His^{93}$ about 5 Å away from Ni, which could help in orientating molecules binding to Ni. Although the lower part of cluster C carrying Fe1, Fe2, and Fe4 is exposed to a mixed hydrophobic-hydrophilic environment with several well-ordered water molecules near Fe1, the upper part near Ni and Fe3 faces the end of a branch of a continuous channel that extends from the surface of the dimer and along all metal clusters (Fig. 4). In the COOH-terminal domain the channel is hydrophobic and is lined by the two middle strands of the central β sheet. The main branch of this putative substrate channel tightens at $Leu^{442}$ and then continues to a positively charged wide channel that harbors more than 40 water molecules. This water deposit is situated close to the clusters B, B′, and D (Fig. 4) near the subunit interface and allows water molecules to enter the active site through an extension of the main branch of the channel. It has two hydrophilic entrance sites for water molecules consumed during CO oxidation nearby (Fig. 4). $CO_2$ could possibly leave the active site in both directions. Shortly after the restriction at $Leu^{442}$, a negatively charged cavity, about 7 Å long, ends directly above the Ni ion of the active site (Fig. 4). A 4.2σ peak in a difference density ($F_{obs} - F_{calc}$) map is situated at the end of the cavity and indicates an unidentified molecule with low occupancy at an apical coordination site ~2.4 Å above the Ni ion.

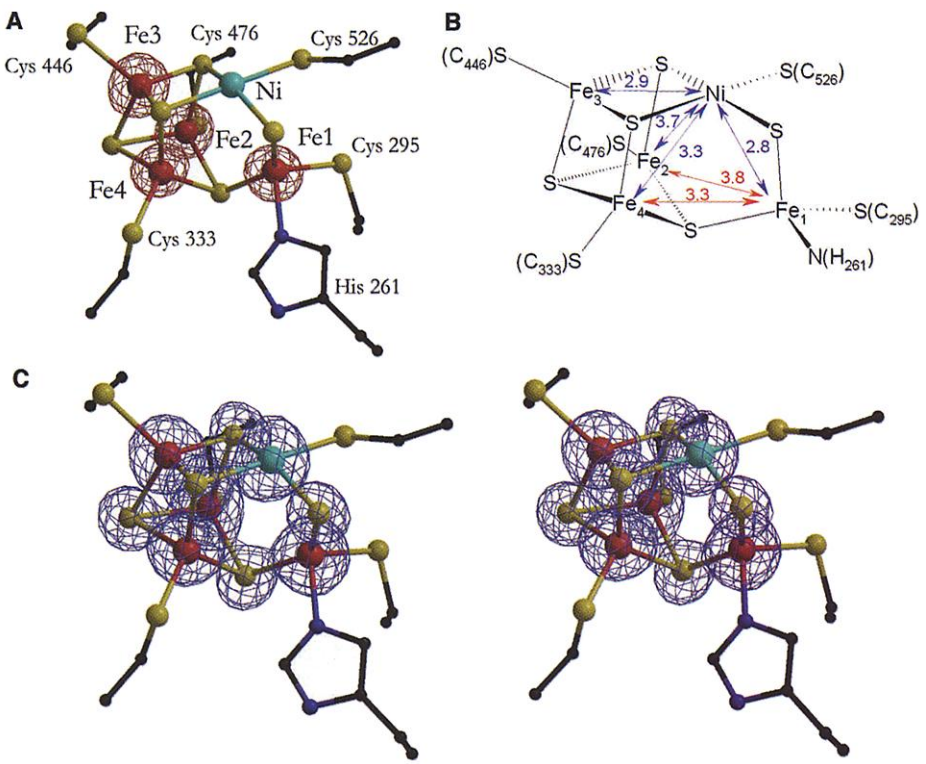


**Fig. 3.** Cluster C, the active site of CO dehydrogenases. (**A**) View of the cofactor with its protein ligands. The identification of Fe and Ni ions in cluster C is based on anomalous difference Fourier maps at λ = 1.7389, 1.5418 (contoured at 4σ and depicted in red) and 1.4856 Å. Although the Fe ions are strong anomalous scatterers at all three wavelengths, the contribution of Ni is weak for the first two wavelengths but strong for the third wavelength. This identification is in agreement with the ligand geometries found for the five metal ions. When the occupancies used for the refinement of cluster C were all set to 0.9 to achieve similar B values for all three clusters, a slightly reduced occupancy for cluster C compared to the other prosthetic groups was found. (**B**) Schematic presentation of cluster C with Ni-Fe (blue) and selected Fe-Fe (red) distances. The short distances between Ni and Fe1 and Ni and Fe3 show additionally the integration of the Ni ion into the cluster. (**C**) Stereo view of 1.63 Å resolution $F_{obs} - F_{calc}$ omit map (blue), contoured at 7σ, calculated for the "inorganic" part of cluster C.

**CO binding and oxidation.** The structure of cluster C in the dithionite-reduced CODH II from *C. hydrogenoformans* does not provide conclusive evidence to identify the exact positions where CO and $H_2O$ would bind. However, several lines of evidence suggest that the major part of the CO oxidation chemistry might involve the neighboring Ni ion and the Fe1 ion of clusters C or C′ in a bimetallic mechanism (Fig. 5A). The Ni ion has an empty apical coordination site external to the cluster and accessible to the substrate channel. ENDOR spectroscopy of the CODH from *C. thermoaceticum* suggested that in the $C_{red1}$ state a hydroxyl-group is donated by a histidine-coordinated Fe ion of cluster C, designated ferrous component II (*16*). In cluster C of the CODH II from *C. hydrogenoformans*, the proximity of the asymmetrically coordinated Fe1 to the Ni ion and its histidine coordination (Fig. 3) suggest that Fe1 could function as a hydroxyl donor for a Ni-bound CO (Fig. 5A). The OH group is absent in the structure of cluster C of CODH II, because the enzyme was investigated in the dithionite-reduced state. According to the structure-based model for the reaction mechanism depicted in Fig. 5A, an incoming CO molecule would bind at the external apical coordination site of the Ni, forming a Ni-carbonyl, which, after a ligand rearrangement, is subject to a nucleophilic attack by a hydroxyl group at Fe1. Protons liberated during the reaction can be absorbed by basic residues in the vicinity of cluster C. Consistent with this hypothesis, con-

served basic residues are found at Lys[563], His[93], and the Fe1-coordinating His[261] (*23*). Oxidation of a Ni-bound CO would leave two electrons at the Ni site, presumably resulting in the intermediate formation of an $Ni^{+}$ ion, which would be paramagnetic. The fact that the Ni ion remains EPR silent under all experimental conditions applied so far with the CODH from *C. hydrogenoformans* (*5*), or from other anaerobic bacteria (*2*, *11*, *24*, *25*), seems to be in conflict with the formation of a Ni-carbonyl. However, the incorporation of Ni into a polynuclear cluster with μ-S ligands might allow significant delocalization of the metal *d* electrons over the ligand orbitals and adjacent Fe atoms. This would favor fast electron withdrawal from Ni or Fe1 by using the [3Fe-3S] subsite of cluster C as an electron sink.

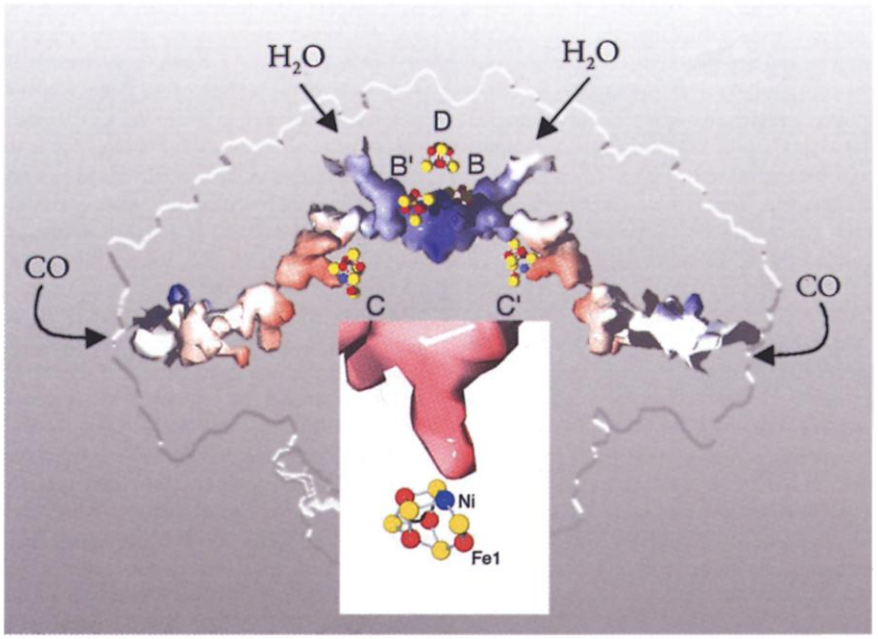


**Fig. 4.** A putative substrate and water channel ranging through the dimer of CODH II. A hydrophobic channel in the COOH-terminal domain of the protein shows a restriction shortly before it reaches the active-site cluster C. A branch of the channel depicted in the inset ends at cluster C directly above the apical coordination site of the Ni ion. The channel continues (as it becomes more hydrophilic) to a positively charged water-filled cavity near the subunit interface. A continuous channel from the surface to the active-site cluster C only became apparent when a small probe of 1.0 Å radius was used in the calculation because of a restriction at Leu[442]. The calculation of the water channel and/or cavity has been carried out with a probe radius of 1.4 Å. Arrows mark the potential entrances for the substrates CO and $H_2O$. The channel mask has been calculated with GRASP (*38*) and was subsequently rendered with POVRAY.

**Intramolecular electron transfer.** The observed spatial arrangement of the five metal clusters in *C. hydrogenoformans* CODH II provides a plausible electron transfer path extending from the buried active site to the molecular surface (Fig. 5B). The mixed-type Ni-Fe clusters C and C′ represent independent active sites, because they are ~33 Å apart from each other. They are the starting points for two separate branches of the electron transport path, which has a junction at cluster D. Electron transfer from cluster C to cluster D involves cluster B′, and electron transfer from cluster C′ to cluster D involves cluster B (Fig. 5B). Thus each branch of the electron transport path is built up by both monomers of the enzyme. In the same monomer, the shortest distances are 28 Å between cluster C and cluster B (or cluster C′ and cluster B′) and 23 Å between cluster C and cluster D (or cluster C′ and cluster D). In the dimer, cluster C of one monomer and cluster B′ of the other monomer (or cluster C′ and cluster B) are only 11 Å apart, allowing an effective transfer of electrons (*26*). The [3Fe-3S] subsite of cluster C (or C′) is orientated toward cluster B′ (or B), which further supports a rearrangement of the initial square-pyramidal Ni coordination into a trigonal-bipyramidal geometry (*18*), which would mainly involve the side chain of Cys[526], could move CO toward the OH, making a nucleophilic attack possible. (**B**) The distances indicate the necessity for electron transfer after CO oxidation from cluster C to cluster B′ (the prime denotes that the cluster is donated by the other subunit), where they can continue to cluster D. Distances of 28 Å between cluster C and B (or cluster C′ and B′) and 23 Å between cluster C and D (or cluster C′ and D) are too long to allow effective electron transfer within the same subunit (*26*).

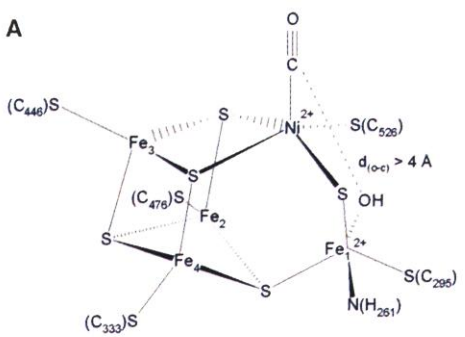


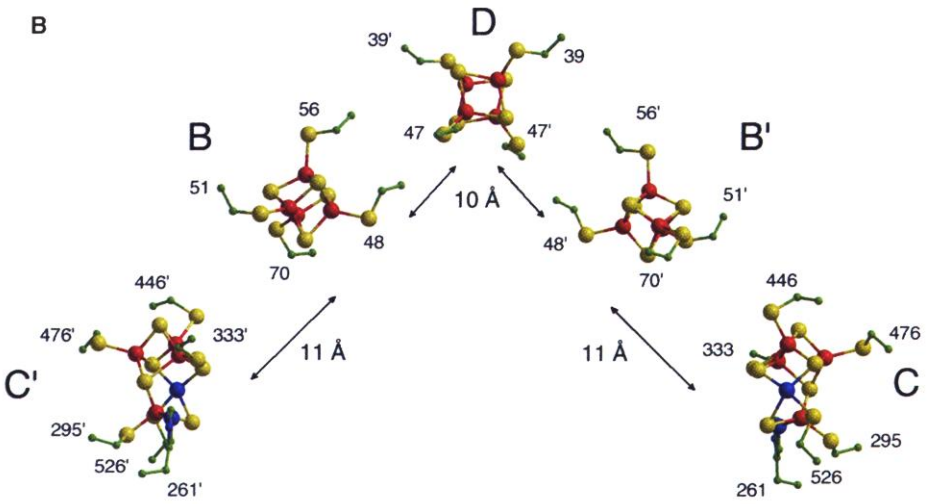


**Fig. 5.** Structure-based model of CO binding and initiation of the CO oxidation reaction at cluster C and pathway for electron transfer. (**A**) The model assumes that an incoming CO molecule binds at the empty and accessible apical coordination site of the square-planar Ni ion. The binding of CO leads to a square-pyramidal ligated Ni ion, a coordination geometry frequently found for pentacoordinated Ni complexes. The binding of CO does not interfere with neighboring atoms, because all closest distances are larger than 3.5 Å. The binding of OH leads to a trigonal-bipyramidal geometry of the pentacoordinated Fe1. This geometry with the OH group bound in *trans* position to His[261] can be achieved by a slight movement of Fe1 by 0.3 to 0.4 Å, which has been assumed in the model. The distances between the OH group and neighboring atoms are larger than 2.6 Å and are not in conflict with the indicated position of the OH group. The CO to OH distance of larger than 4 Å does not allow interaction.

ports the direction of electron transfer (Fig. 5B). From cluster B′ (or B), electron transfer continues to cluster D, which is a 10 Å distance away. As cluster D is exposed to the solvent, it can allow facile electron transfer to external acceptors.

The proposed intramolecular electron path is supported by functional evidence. EPR of the *C. hydrogenoformans* CODH has suggested the presence of at least two different redox active [4Fe-4S] clusters (*5*). A rhombic signal obtained at 10 to 25 K with $g_{av} = 1.94$ was interpreted to originate from a $[4Fe\text{-}4S]^{1+}$ cluster similar to the reduced electron-transferring cluster B of the CODHs from *R. rubrum* or *C. thermoaceticum*. Another rhombic signal appearing at 10 K and absent at 25 K with $g_{av} = 1.84$ was believed to come from a faster-relaxing $[4Fe\text{-}4S]^{1+}$ cluster similar to the fully reduced CO-oxidizing cluster C of the CODHs from *R. rubrum* or *C. thermoaceticum*.

**CODH of *C. hydrogenoformans* is the prototype for Ni-containing CODHs.** CODH II from *C. hydrogenoformans* exhibits extended sequence similarity to Ni CODHs from anaerobic phototrophic, acetogenic, sulfate-reducing, and methanogenic bacteria and archaea, as well as to the hybrid-cluster protein (HCP) from different sources, suggesting similarity in global folding of these proteins (*23*).

The amino acids 150 to 637 of CODH II are 23% identical to the amino acids 139 to 553 of HCP (*23*), a metalloprotein of unknown function from *Desulfovibrio vulgaris* (*27*), which contains an unusual hybrid cluster. The database search program DALI (*28*) reveals a highly homologous structure (Z score of 22.5) in HCP. Like CODH II subunit (637 residues), the HCP (553 residues) monomer has three domains. Structural homology between the two proteins extends over all three domains, but is most striking in the middle and COOH-terminal domains that contain similar Rossman-type folds. The $NH_2$-terminal domain of HCP contains two three-helix bundles in contrast to the single three-helix bundle in CODH II. HCP contains two Fe-S clusters. Cluster 1 is a conventional [4Fe-4S] cubane-type, and cluster 2 an asymmetric, open structured hybrid [4Fe-2S-2O] cluster (*29*). The cubane-type [4Fe-4S] cluster of HCP resides in the first three-helix bundle of the $NH_2$-terminal domain, which is missing in CODH II (Fig. 2). The orientation of the three-helix bundle in the CODH II dimer is similar to the orientation of the two bundles in HCP, so that cluster B′ occupies a similar position (Fig. 1). A structural alignment of the sequences from both proteins reveals that the position of the residues binding cluster C and those binding the hybrid-cluster are mostly conserved, although their roles and features are apparently adapted to coordinate different types of Fe-containing clusters. Although the hybrid-cluster and cluster C differ in essential characteristics, such as arrangement and type of metal ligands, both show an open spatial arrangement of their Fe atoms with one Fe position coordinated by histidine, indicating a possible evolutionary relationship.

Residues coordinating cluster C (motif $His^{261}X_{33}Cys^{295}X_{37}Cys^{333}X_{112}Cys^{446}X_{29}Cys^{476}X_{49}Cys^{526}$; consensus $HisX_{27-35}CysX_{37-38}CysX_{93-197}CysX_{27-29}CysX_{24-49}Cys$), cluster B (motif $Cys^{48}X_2Cys^{51}X_4Cys^{56}X_{13}Cys^{70}$; consensus $CysX_{1-2}CysX_4CysX_{9-14}Cys$) or cluster D (half motif $Cys^{39}X_7Cys^{47}$; consensus $Cys\text{-}X_{2-7}Cys$) in CODH II from *C. hydrogenoformans* are highly conserved in all other known Ni CODHs with very rare conservative exchanges (*23*). The structural and sequence data presented here, along with previous spectroscopic evidence (*2*, *10*, *16*), indicate that all known Ni-containing CODHs from anaerobic bacteria and archaea essentially use the same three metal clusters identified in the CODH II from *C. hydrogenoformans* for $CO/CO_2$ redox catalysis: Cluster C is the active site for $CO/CO_2$ redox chemistry, cluster B mediates the electron transfer from cluster C to cluster D, and cluster D functions in transferring electrons between cluster B and external redox agents.

### References and Notes


1. J. G. Ferry, *Annu. Rev. Microbiol.* **49**, 305 (1995).
2. S. W. Ragsdale, M. Kumar, *Chem. Rev.* **96**, 2515 (1996).
3. O. Meyer *et al.*, *Biol. Chem.* **381**, 865 (2000).
4. V. Svetlitchnyi *et al.*, *Syst. Appl. Microbiol.* **14**, 254 (1991).
5. V. Svetlitchnyi, C. Peschel, G. Acker, O. Meyer, *J. Bacteriol.*, in press.
6. U. Ermler, W. Grabarse, S. Shima, M. Goubeaud, R. K. Thauer, *Curr. Opin. Struct. Biol.* **8**, 749 (1998).
7. H. Dobbek, L. Gremer, O. Meyer, R. Huber, *Proc. Natl. Acad. Sci. U.S.A.* **96**, 8884 (1999).
8. P. Hänzelmann, H. Dobbek, L. Gremer, R. Huber, O. Meyer, *J. Mol. Biol.* **301**, 1221 (2000).
9. J. M. Gonzalez, F. T. Robb, *FEMS Microbiol. Lett.* **191**, 243 (2000).
10. Z. Hu *et al.*, *J. Am. Chem. Soc.* **118**, 830 (1996).
11. C. R. Staples *et al.*, *J. Am. Chem. Soc.* **121**, 11034 (1999).
12. J. Heo, C. R. Staples, C. M. Halbleib, P. W. Ludden, *Biochemistry* **39**, 7956 (2000).
13. CODH II purified from CO-grown *C. hydrogenoformans* (*5*) was obtained at a specific activity of 14 mmol CO oxidized per minute per mg protein. Because of the pronounced oxygen sensitivity of the enzyme, all manipulations during purification, crystallization, and data collection were carried out under anoxic conditions under a flow of $N_2$, or in an anoxic glove box chamber under an atmosphere of pure $N_2$. Crystallization was performed at 23°C using the hanging drop vapor diffusion method. Crystals of CODH II were obtained by mixing 6 μl of protein (16.1 mg protein/ml) in 20 mM Tris/HCl (supplemented with 3 mM sodium dithionite), pH 7.5, with 3 μl of reservoir solution, containing 20% (vol/vol) 2-propanol, 20% (wt/vol) polyethylene glycol 3000 (PEG 3000), and 100 mM Hepes/NaOH, pH 7.5. Crystals, which appeared within about 24 hours, were shock-frozen in reservoir solution supplemented with 5% glycerol and 5 mM sodium dithionite, and stored frozen in liquid nitrogen. Rapid crystallization and immediate freezing of crystals kept under anoxic conditions were mandatory to characterize a fully catalytically competent enzyme. The crystal structure of CODH II has been solved by MAD methods using the anomalous scattering of iron. The enzyme crystallized in the monoclinic spacegroup C2 with cell parameters of $a = 112.2$ Å, $b = 75.1$ Å, $c = 71.1$ Å, and $\beta = 111.2°$, with one monomer per asymmetric unit and a solvent content of about 31%. The position of the iron-sulfur clusters has been determined after a MAD experiment at three different wavelengths at the BM14 (ESRF, Grenoble, France) by difference Patterson methods using the program SOLVE (*30*). Phases calculated with the program SHARP (*31*) and modified with RESOLVE (*32*) allowed the positioning of individual iron atoms for the cubane-type [4Fe-4S] clusters of a CODH II monomer in anomalous difference Fourier maps. Interpretable density maps were obtained by individual refinement of 6 out of 10 Fe atoms in the asymmetric unit and subsequent solvent flattening (Table 1). After building the polypeptide chain, the additional metal sites of cluster C have been located based on Bijvoet and $2F_{obs} - F_{calc}$ maps. Several cycles of manual building with MAIN (*33*), and positional and temperature-factor refinement with CNS (*34*), were followed by one cycle in which SHELX (*35*) was used to refine anisotropic temperature factors for Fe, Ni, and S atoms. The model has been refined to 1.63 Å resolution yielding a model with $R_{cryst}$ of 0.161 and $R_{free}$ of 0.209 and a good stereochemistry.
14. H. Sticht, P. Roesch, *Progr. Biophys. Mol. Biol.* **70**, 95 (1998).
15. N. J. Spangler *et al.*, *J. Biol. Chem.* **273**, 4059 (1998).
16. V. J. DeRose, J. Telser, M. E. Anderson, P. A. Lindahl, B. M. Hoffman, *J. Am. Chem. Soc.* **120**, 8767 (1998).
17. M. Kumar, W. Lu, L. Liu, S. Ragsdale, *J. Am. Chem. Soc.* **115**, 11646 (1993).
18. C. L. Coyle, E. I. Stiefel, in *The Bioinorganic Chemistry of Nickel* J. R. J. Lancaster, Ed. (VCH Publishers, New York, 1988), pp. 1–28.
19. H. Beinert, *J. Biol. Inorg. Chem.* **5**, 2 (2000).
20. M. K. Johnson, *Curr. Opin. Chem. Biol.* **2**, 173 (1998).
21. B. R. Crane, L. M. Siegel, E. D. Getzoff, *Science* **270**, 59 (1995).
22. J. W. Peters, W. N. Lanzilotta, B. J. Lemon, L. C. Seefeldt, *Science* **282**, 1853 (1998).
23. A sequence alignment of CODH II with selected homologous proteins is available as supplemental data on *Science* Online at www.sciencemag.org/cgi/content/full/293/5533/1281/DC1.
24. D. Bonam, P. W. Ludden, *J. Biol. Chem.* **262**, 2980 (1987).
25. J. Heo, C. R. Staples, J. Telser, P. W. Ludden, *J. Am. Chem. Soc.* **121**, 11045 (1999).
26. C. C. Page, C. C. Moser, X. Chen, P. L. Dutton, *Nature* **402**, 47 (1999).
27. A. F. Arendsen *et al.*, *J. Biol. Inorg. Chem.* **3**, 81 (1998).
28. L. Holm, C. Sander, *J. Mol. Biol.* **233**, 123 (1993).
29. A. F. Arendsen, P. F. Lindley, in *Iron-Sulfur Proteins*, A. G. Sykes, Ed. (Academic Press, San Diego, 1999), vol. 47, pp. 219–249.
30. T. C. Terwilliger, J. Berendzen, *Acta Crystallogr. D* **55**, 849 (1999).
31. E. de La Fortelle, J. J. Irwin, G. Bricogne, *Crystallogr. Comput.* **7**, 1 (1997).
32. T. C. Terwilliger, *Acta Crystallogr. D* **56**, 965 (2000).
33. D. Turk, thesis, Technische Universität München, Munich (1992).
34. A. T. Brünger *et al.*, *Acta Crystallogr. D* **54**, 905 (1998).
35. G. M. Sheldrick, T. R. Schneider, *Methods Enzymol.* **277**, 319 (1997).
36. R. M. Esnouf, *J. Mol. Graph.* **15**, 132 (1997).
37. D. J. Bacon, W. F. Anderson, *J. Mol. Graph.* **6**, 219 (1988).
38. A. Nicholls, R. Bharadwaj, B. Honig, *Biophys. J.* **64**, A166 (1993).


39. We thank G. Leonard at the BM14, ESRF, Grenoble for his help in data collection and multiwavelength anomalous diffraction measurements and M. Frey (Université Joseph Fourier), H. Drake (Universität Bayreuth), and A. Wolf (Universität Bayreuth) for reading the manuscript. This work was financially supported by the Fonds der Chemischen Industrie (Frankfurt am Main, Germany). Coordinates have been deposited at the Protein Data Bank (accession code 1JJY).

10 April 2001; accepted 10 July 2001